Electrical Engineering Research Laboratory
The University of Texas

EERL 3-24 CF-2847

REFLECTING CHARACTERISTICS OF POGO PARACHUTE MODELS D556, D503-6 and P/N 509-330

By

C. O. Britt

L. C. Krause

W. W. Bahn

20 January 1960 Copy No. 81

A Technical Report Prepared Under U. S. Navy
Bureau of Naval Weapons (Bureau of Ordnance)
Contract NOrd 16498, Task UTX-1
Problem UTX-1-D-3

29

ELECTRICAL ENGINEERING RESEARCH LABORATORY

THE UNIVERSITY OF TEXAS

EERL 3-24 CF-2847

REFLECTING CHARACTERISTICS OF POGO PARACHUTE MODELS D 556, D 503-6 and P/N 509-330

By

C. O. Britt
L. C. Krause
W. W. Bahn

20 January 1960 Copy No. 81

A Technical Report Prepared Under U. S. Navy
Bureau of Naval Weapons (Bureau of Ordnance)
Contract NOrd 16498, Task UTX-1
Problem UTX-1-D-3

Initial distribution of this document has been made in accordance with the list for guidance published in APL/JHU TG 8-11, dated November 1953. Copies 110-125 retained for Electrical Engineering Research Laboratory internal use.

TABLE OF CONTENTS

LIST OF FIGURES

ABSTRACT

This report contains the measured radar scattering cross sections of three model POGO parachutes, designated as D 503-6, D 556 and P/N 509-330. Observations made with 1/6 scale models will permit the results to be scaled from a modeling frequency of 35 kmcs to a simulated frequency of 5.83 kmcs.

I. INTRODUCTION

These measurements were made for the purpose of providing data for the Physical Science Laboratory of the State College of New Mexico under Bureau of Ordnance Contract 16498, Task UT-1-D-2, coordinated by the Applied Physics Laboratory of Johns Hopkins University. A 35 kmcs range-gated radar was used to measure the scattering cross-section of three each 1/6 scale parachute models. The parachutes are designated as D 556, D 503-6 and P/N 509-330. The technique of measuring the scale models has been previously described.[1]

II. SCATTERING CROSS-SECTIONS

Model parachute D 556 and the "mechanical monkey" used to attach the models to the suspension system are shown in figure 1. Two different inflating arrangements of the balloon used with parachute model D 503-6 and

parachute model P/N 509-330 attached to the suspension system are shown in figures 2 and 3.

The models were rotated at a speed of 1 rpm with the axis of rotation in the plane of the parachute's equator. Variations in the rotational speed, caused by changes in wind loading on the models, produced some distortion of the fine scattering lobe structure. The widths of the fine lobes, however, are in general narrow and their exact position problematical relative to the 10 degree increments at which the measurements were requested. The mean of the scattering cross-sections was therefore determined. This was implemented by the triple pattern overlays shown in figures 4 through 15. Shown in figures 16, 17 and 18 are the mean values of the scattering cross-sections of the three parachutes as seen from the transmitter for transmitter-receiver separation angles of 0, 10, 20 and 30 degrees. Deviations from the mean scattering cross-sections that were caused by the fine lobe structures are designated as scintillation.

The scattering cross-sections were derived from figures 16, 17 and 18 for transmitter illuminating angles of 0, 10, 20 and 30 degrees above and below the parachute equators as seen with a receiver whose angle of separation varies from 0 to 10 degrees with respect to the transmitter. These cross-sections are shown in figures 19, 20 and 21.

REFERENCE

1. Tolbert, C. W. and C. O. Britt, "Measured Scattering Cross-Section of Model POGO Parachutes," Report No. 3-23, Electrical Engineering Research Laboratory, The University of Texas, 31 July 1957 (CM-908).

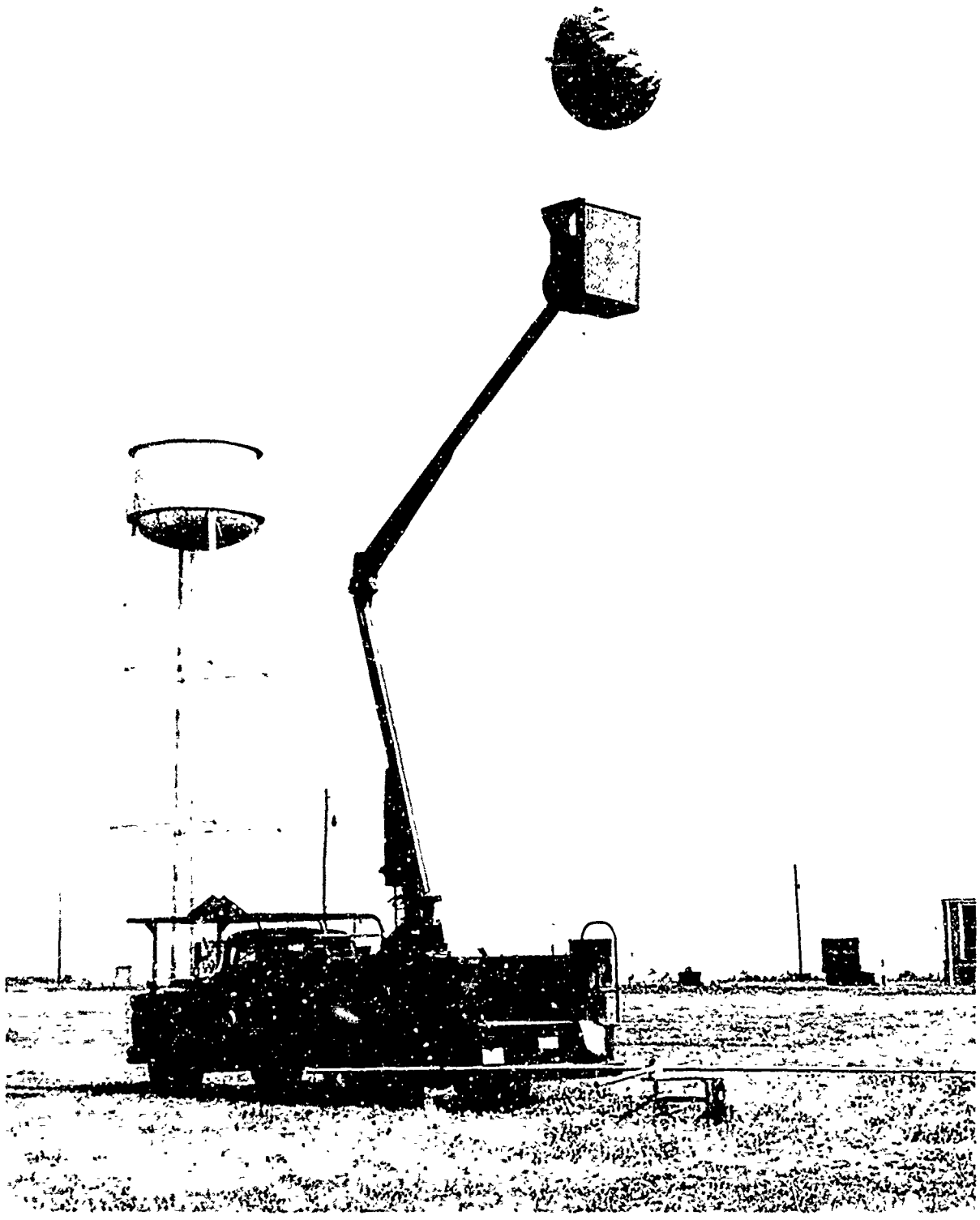

MODEL D-556

FIG. 1

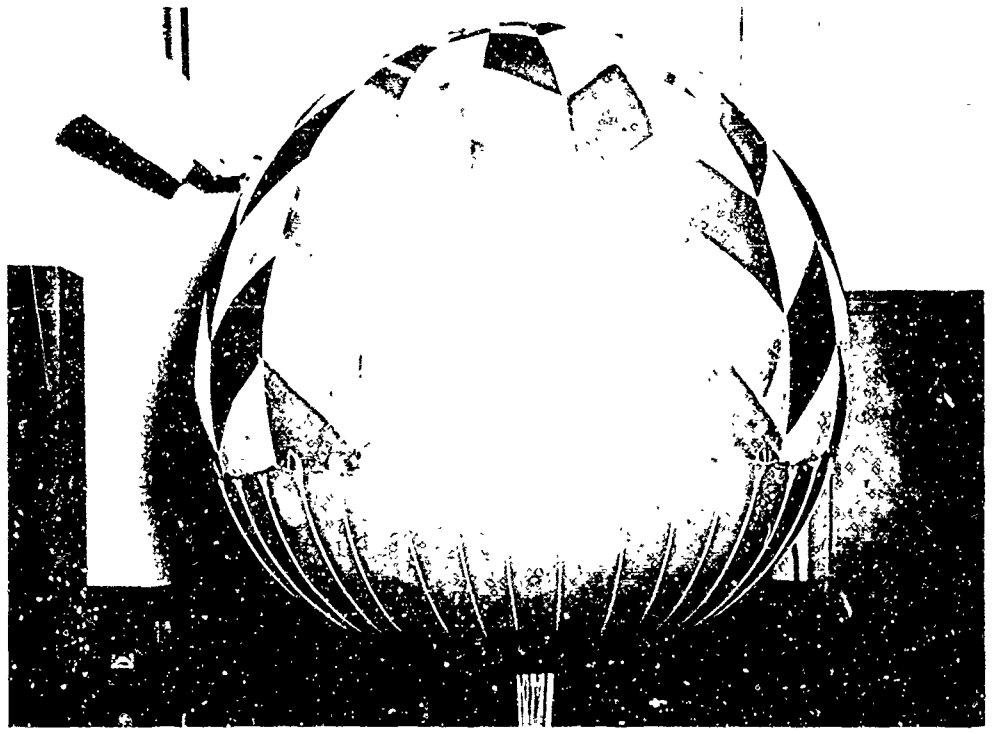

MODEL D-503-6

FIG 2

MODEL P/N 509-330

FIG 3

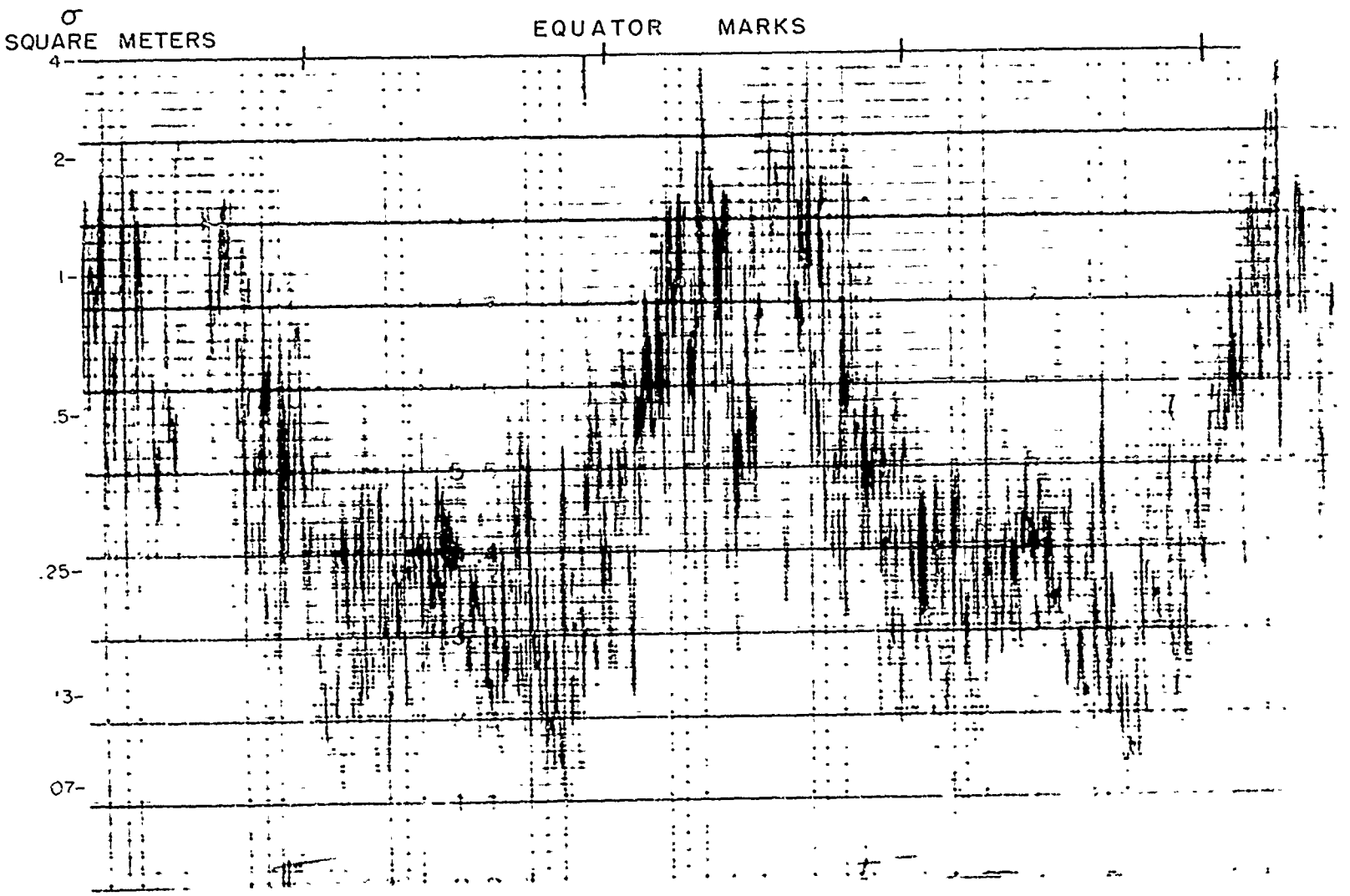

MODEL PARACHUTE D-556 TRANS. 0° REC. 0°

FIG. 4

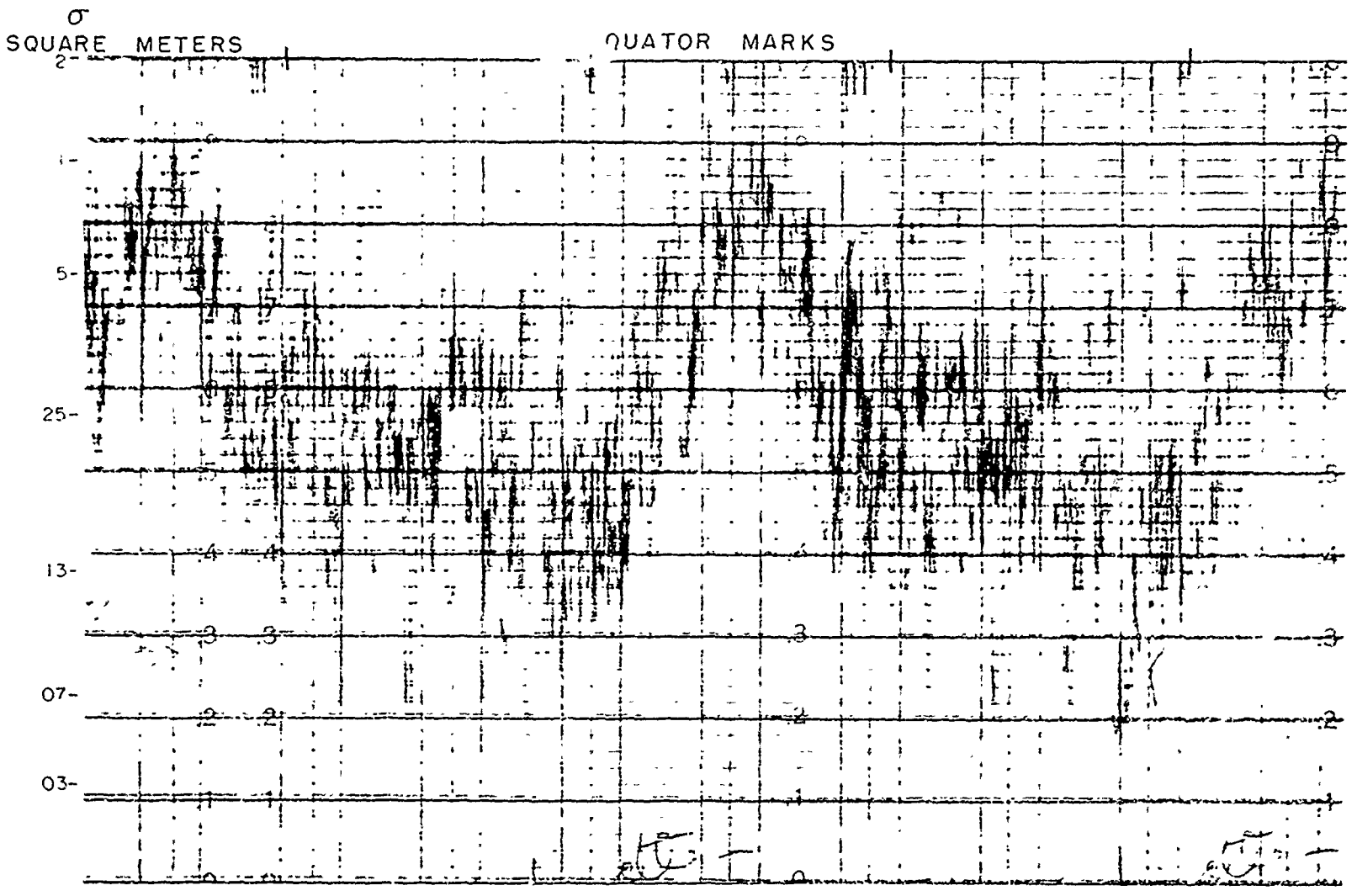

MODEL PARACHUTE D-556 TRANS. 0° REC. 10°

FIG. 5

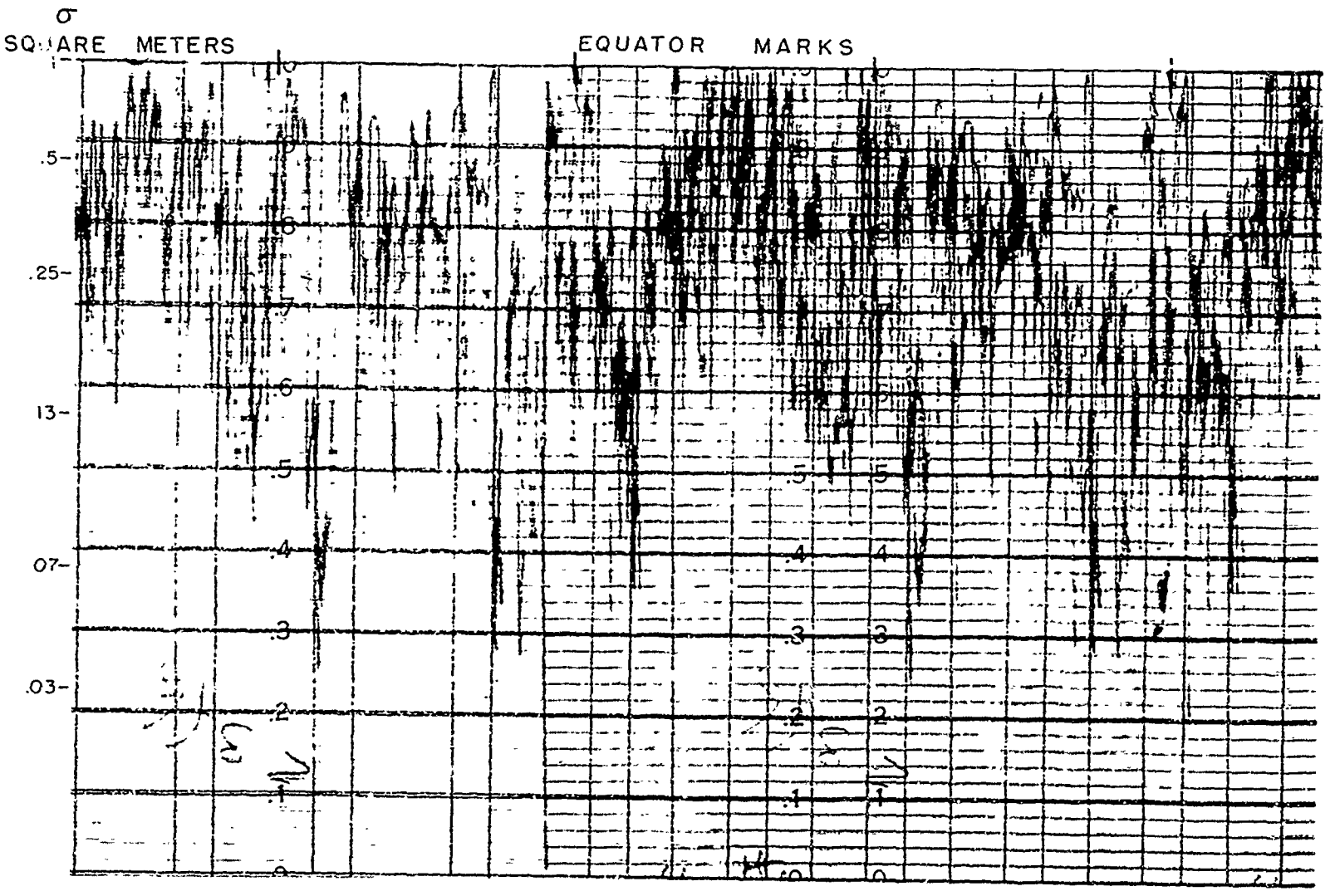

MODEL PARACHUTE D-556 TRANS. 0° REC. 20°

FIG. 6

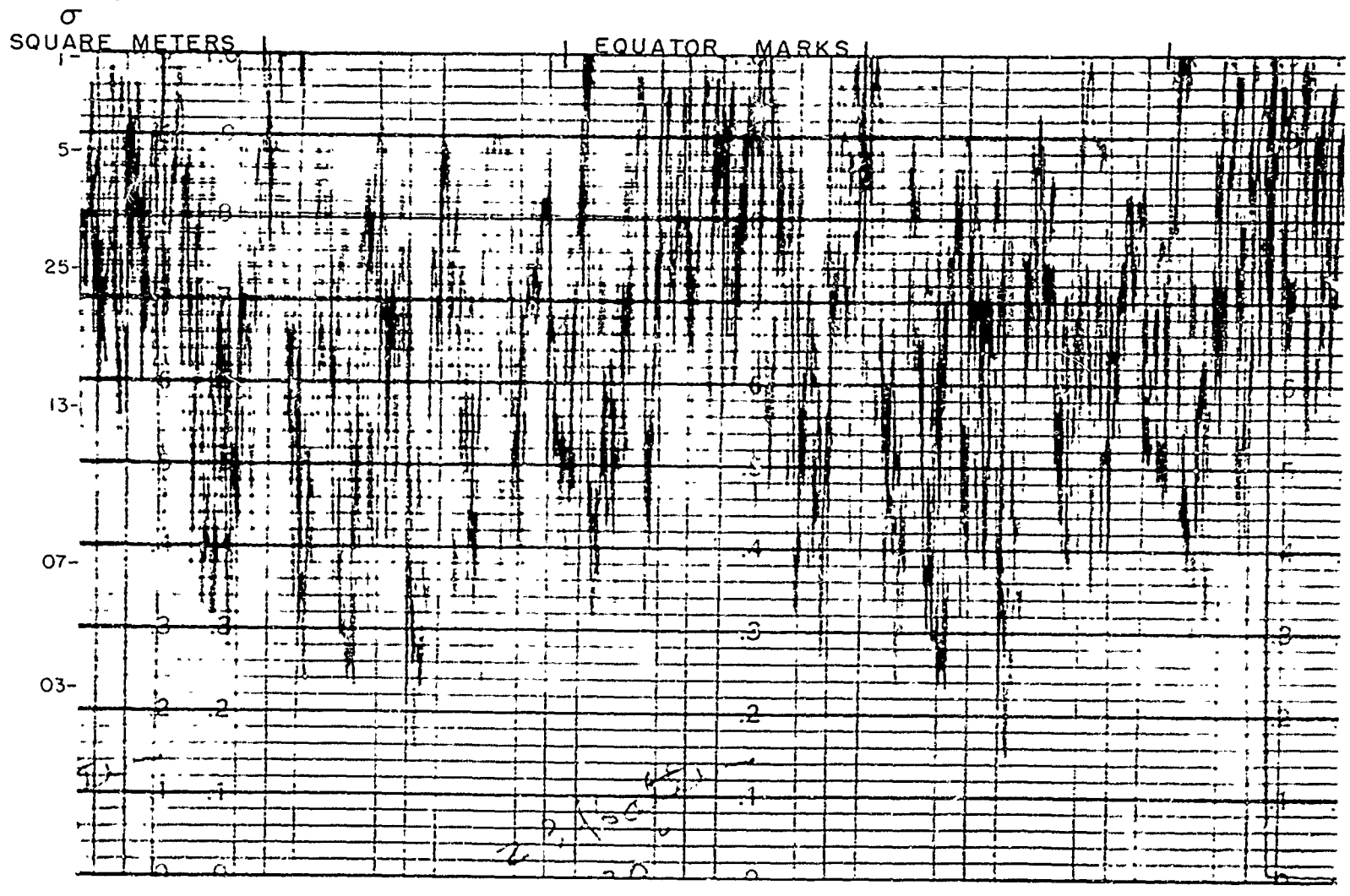

MODEL PARACHUTE D-556 TRANS. 0° REC. 30°

FIG. 7

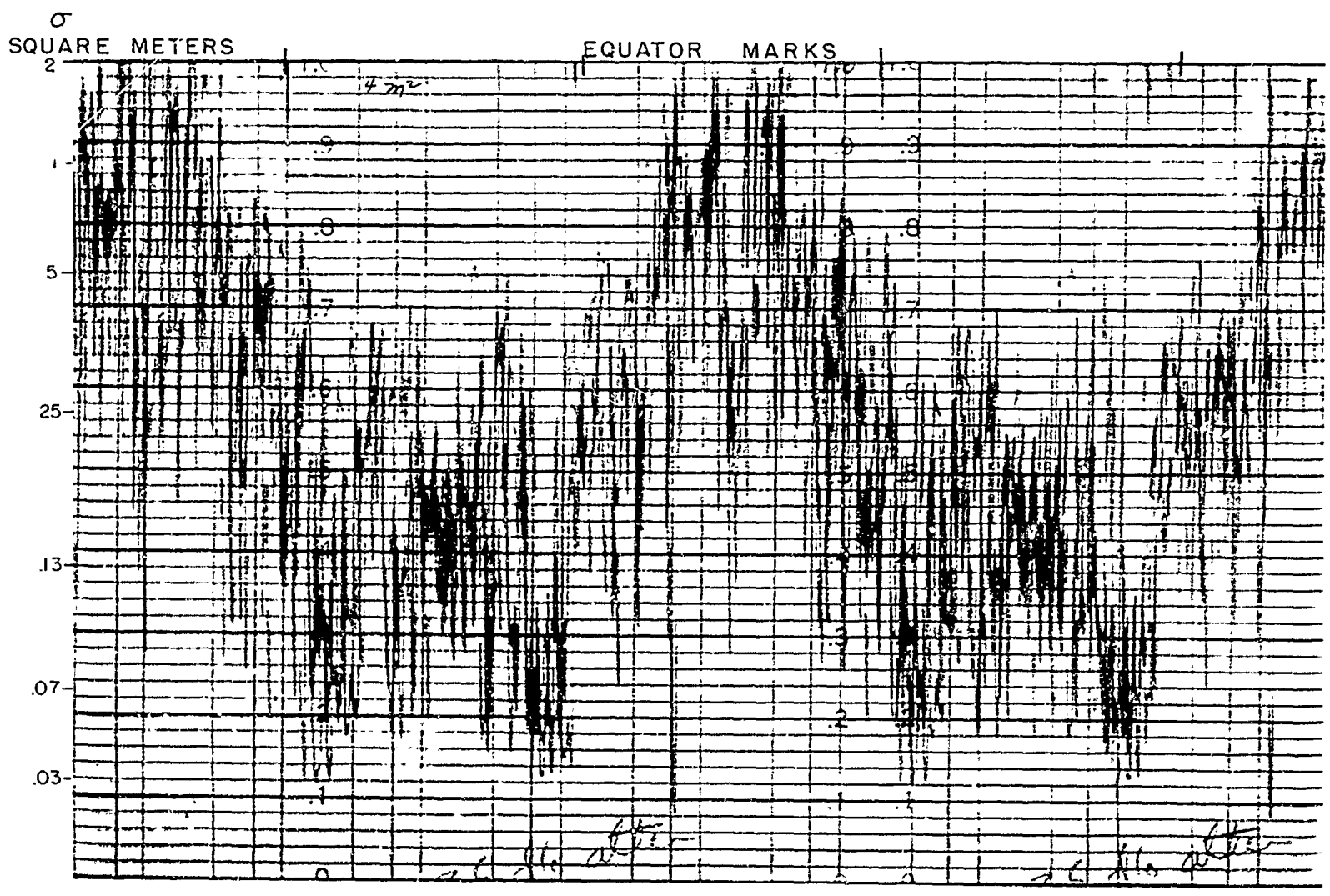

MODEL PARACHUTE D-503-6 TRAN. 0° REC. 0°

FIG. 8

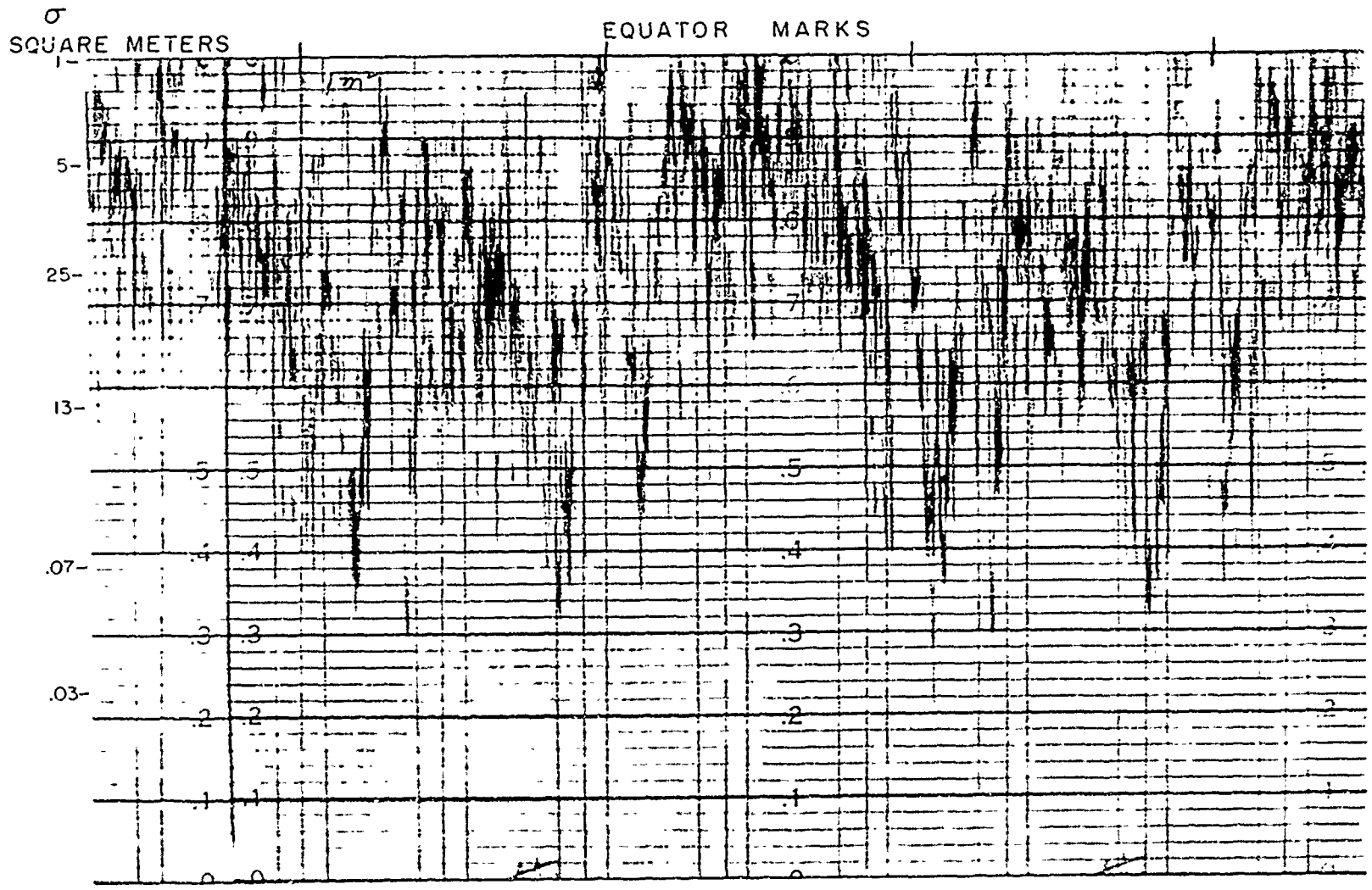

MODEL PARACHUTE D-503-6 TRAN. 0° REC. 10°

FIG. 9

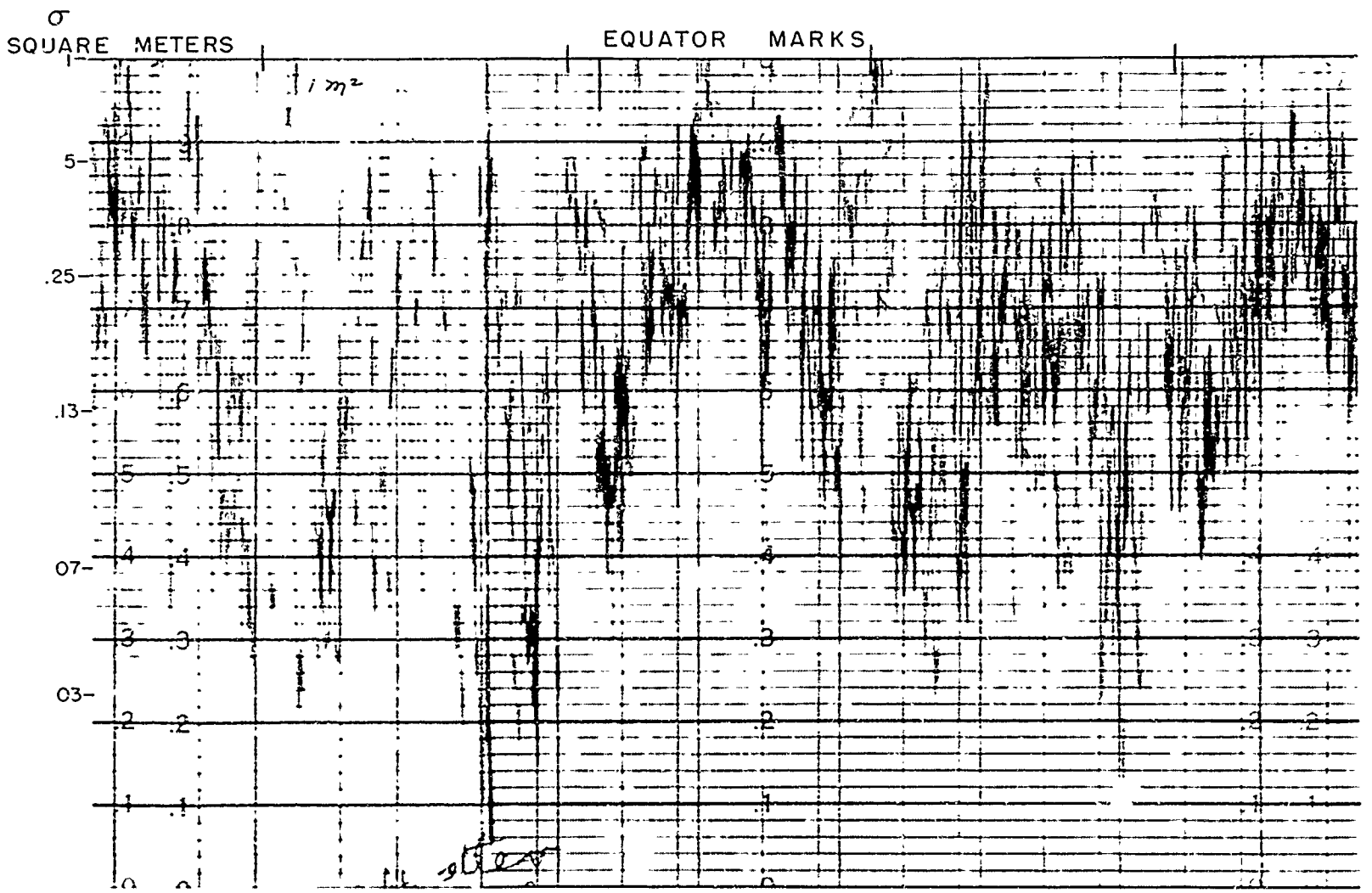

MODEL PARACHUTE D-503-6 TRANS. 0° REC. 20°

FIG. 10

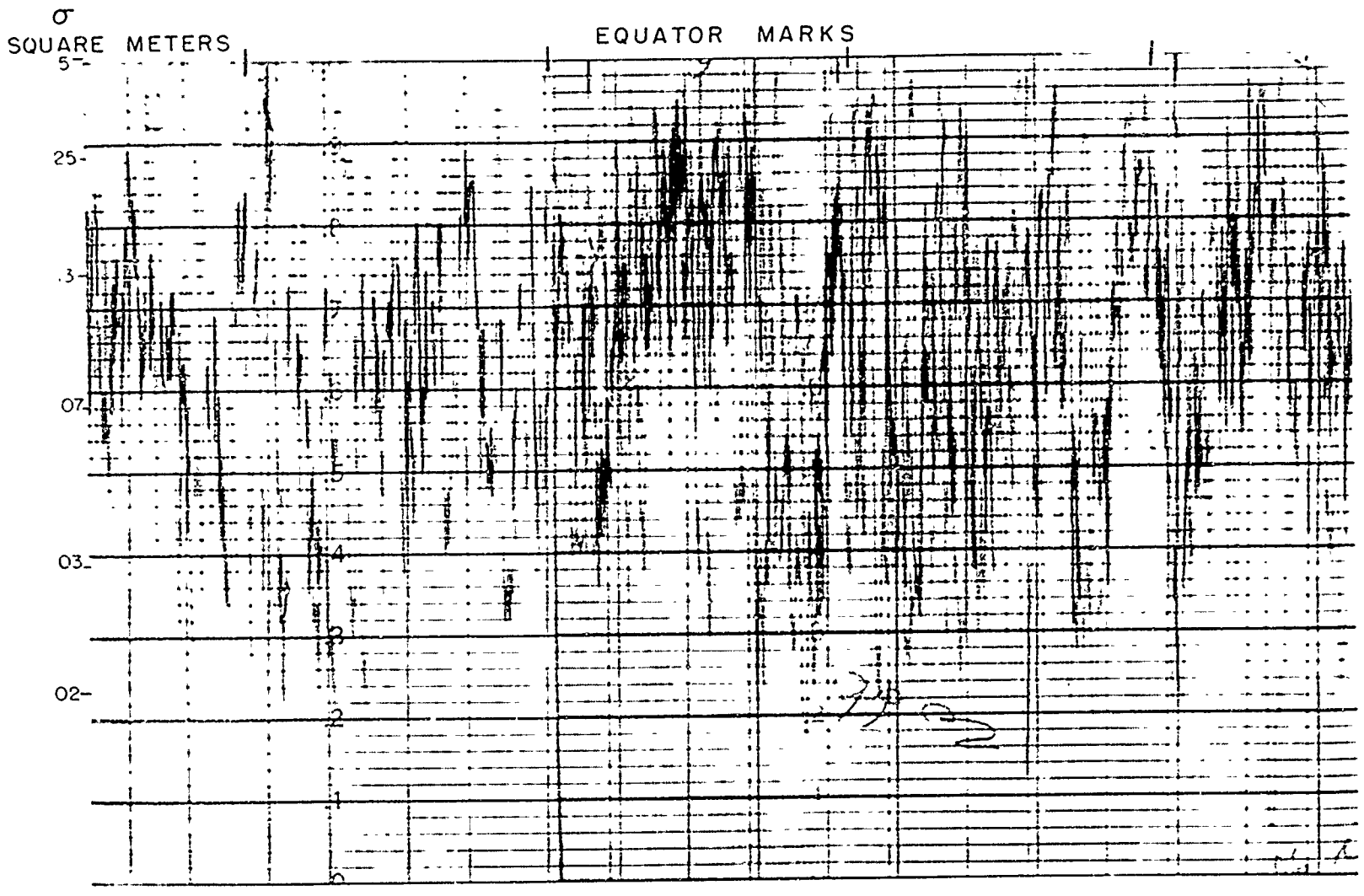

MODEL PARACHUTE D-503-6 TRANS. 0° REC. 30°

FIG. 11

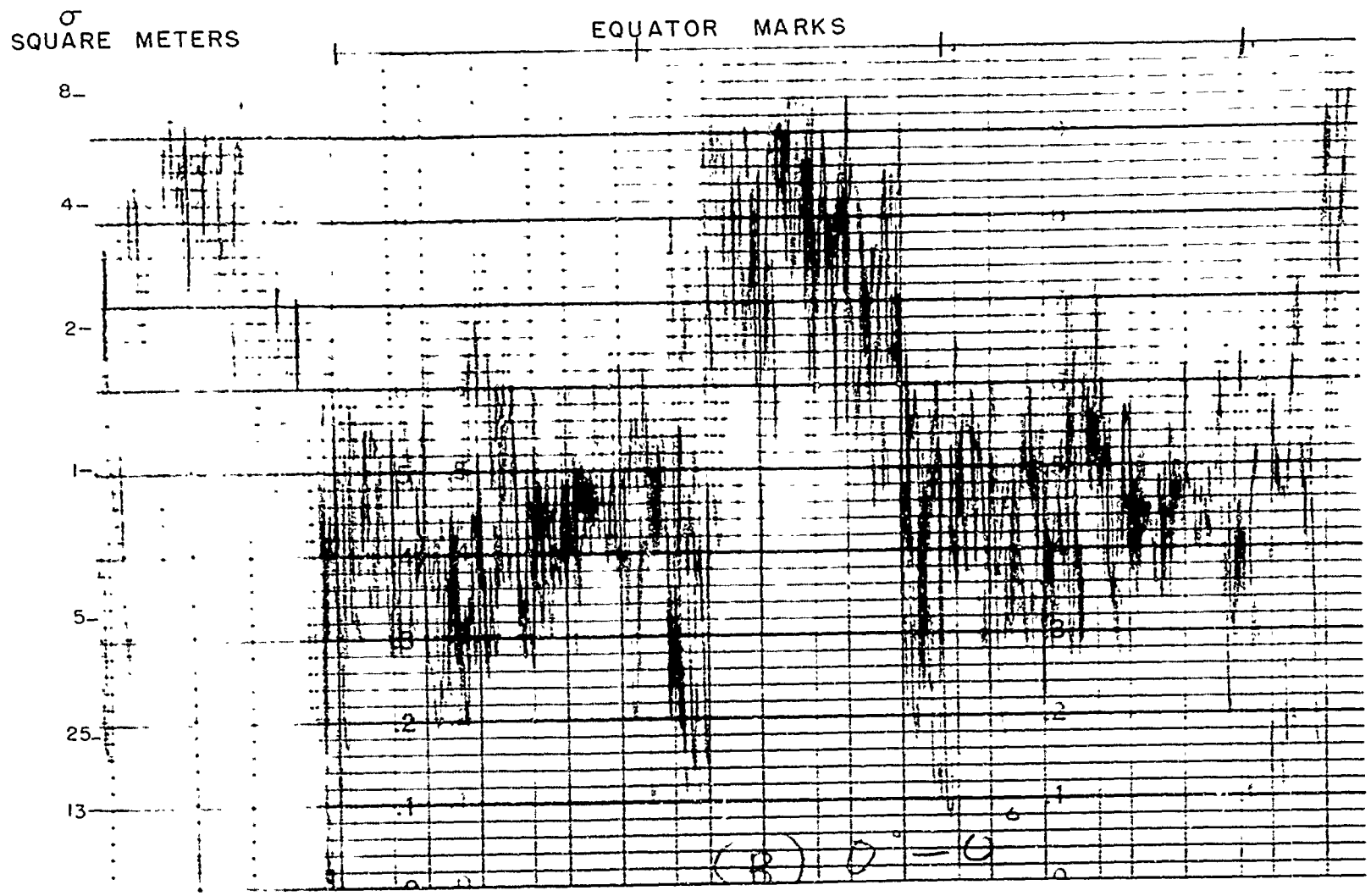

MODEL PARACHUTE P/N 509-330 TRANS. 0° REC 0°

FIG. 12

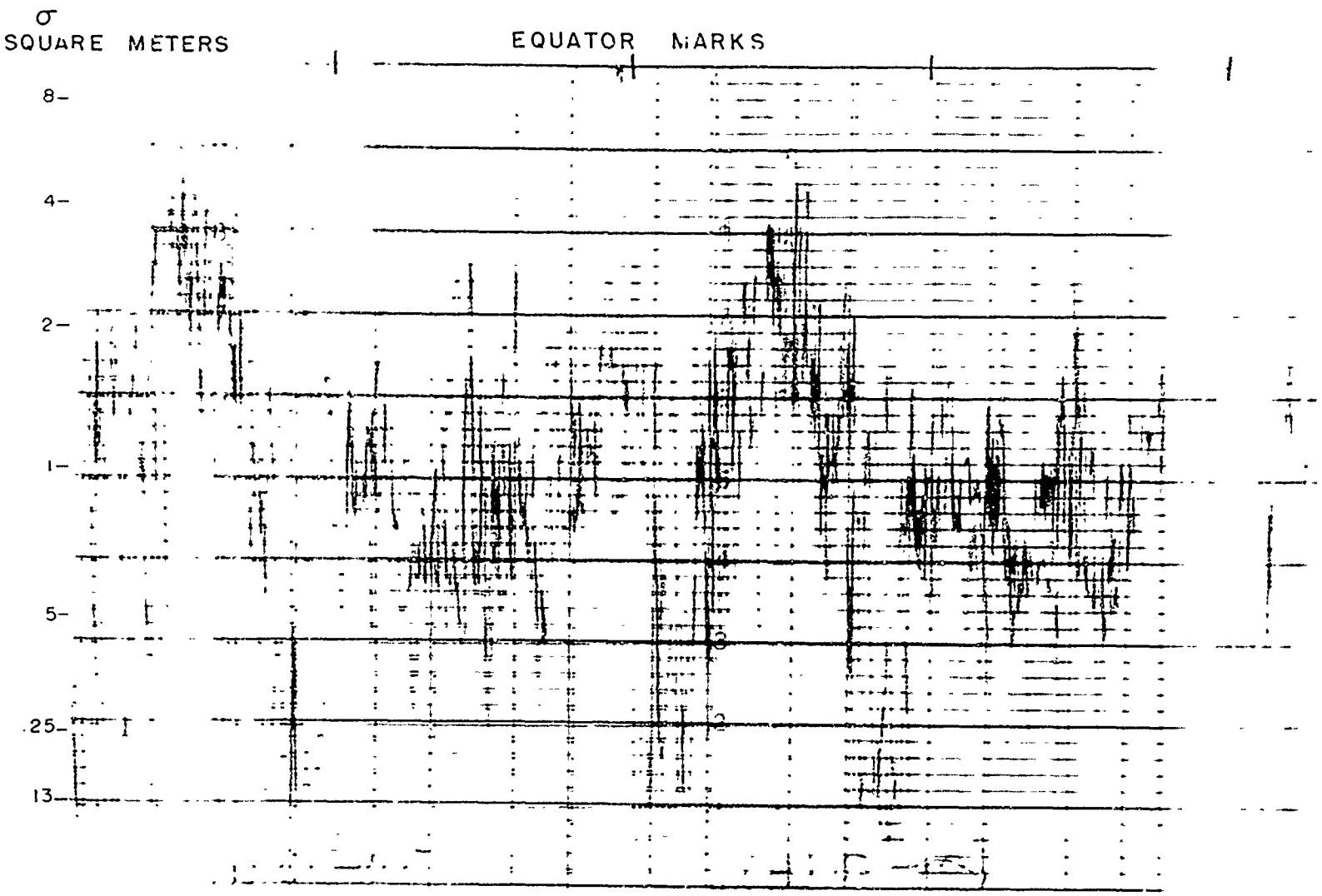

MODEL PARACHUTE P/N 509-330 TRANS. 0° REC. 10°

FIG. 13

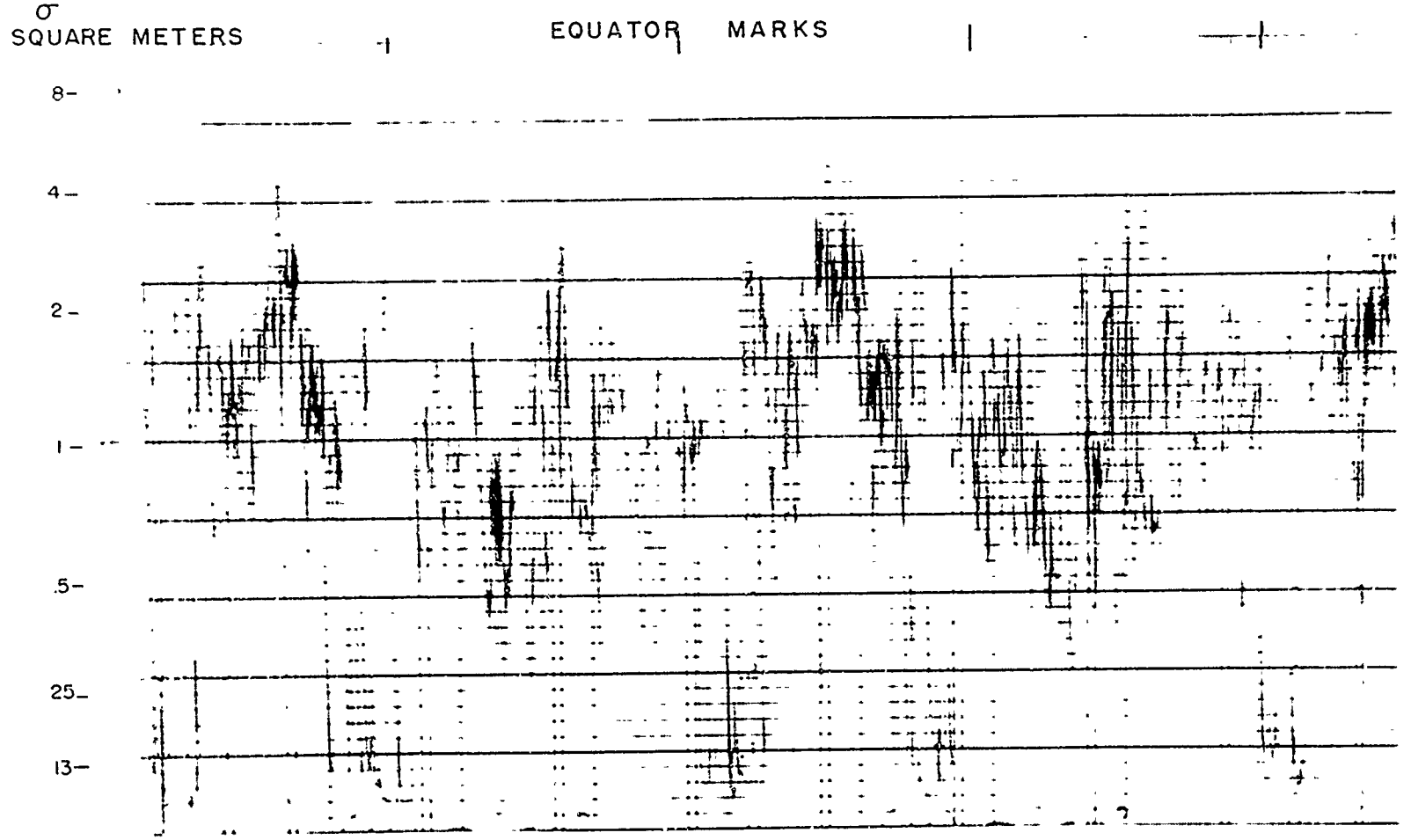

MODEL PARACHUTE P/N 509-330 TRANS. 0° REC. 20°

FIG. 14

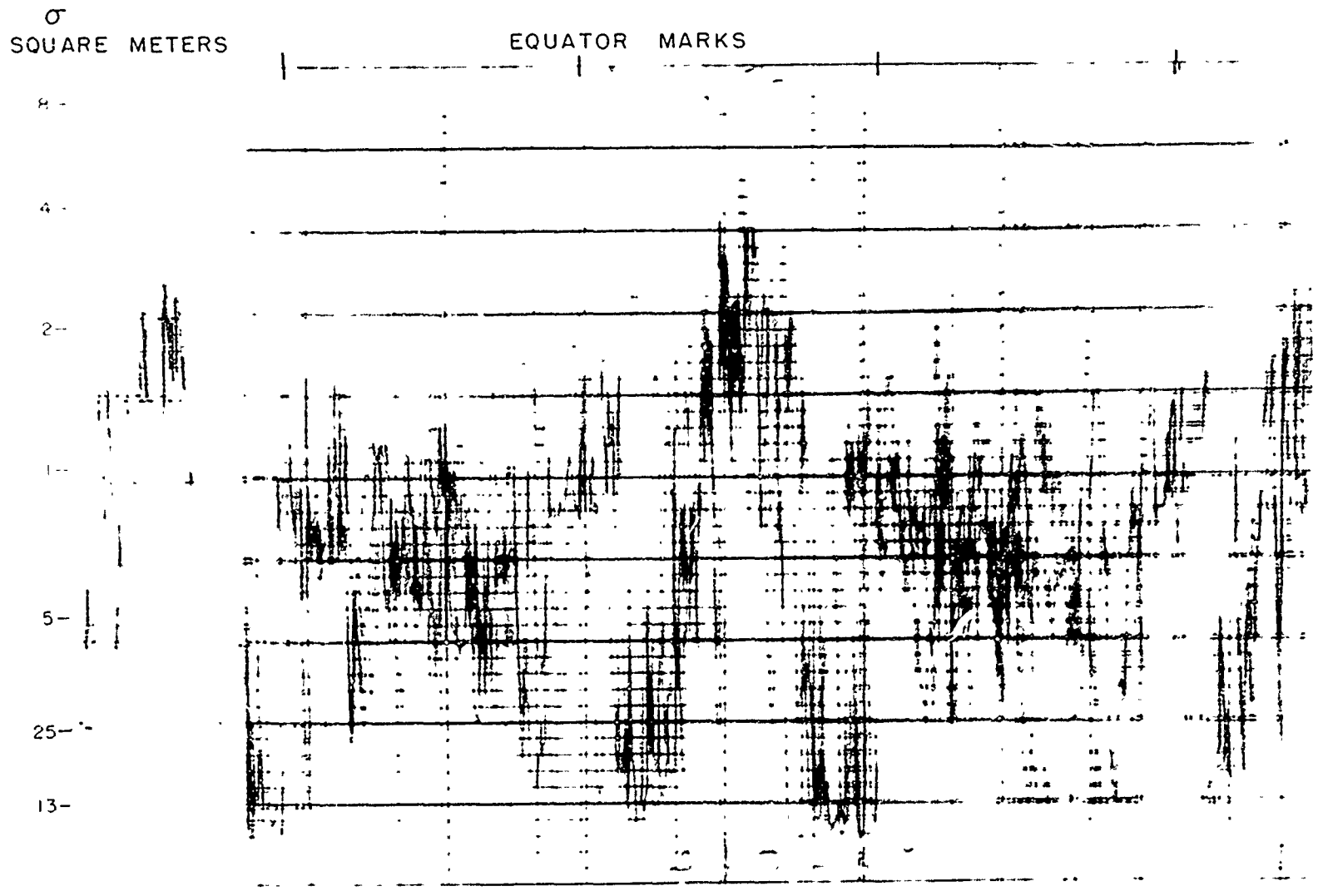

MODEL PARACHUTE P/N 509-330 TRANS. 0° REC. 30°

FIG. 15

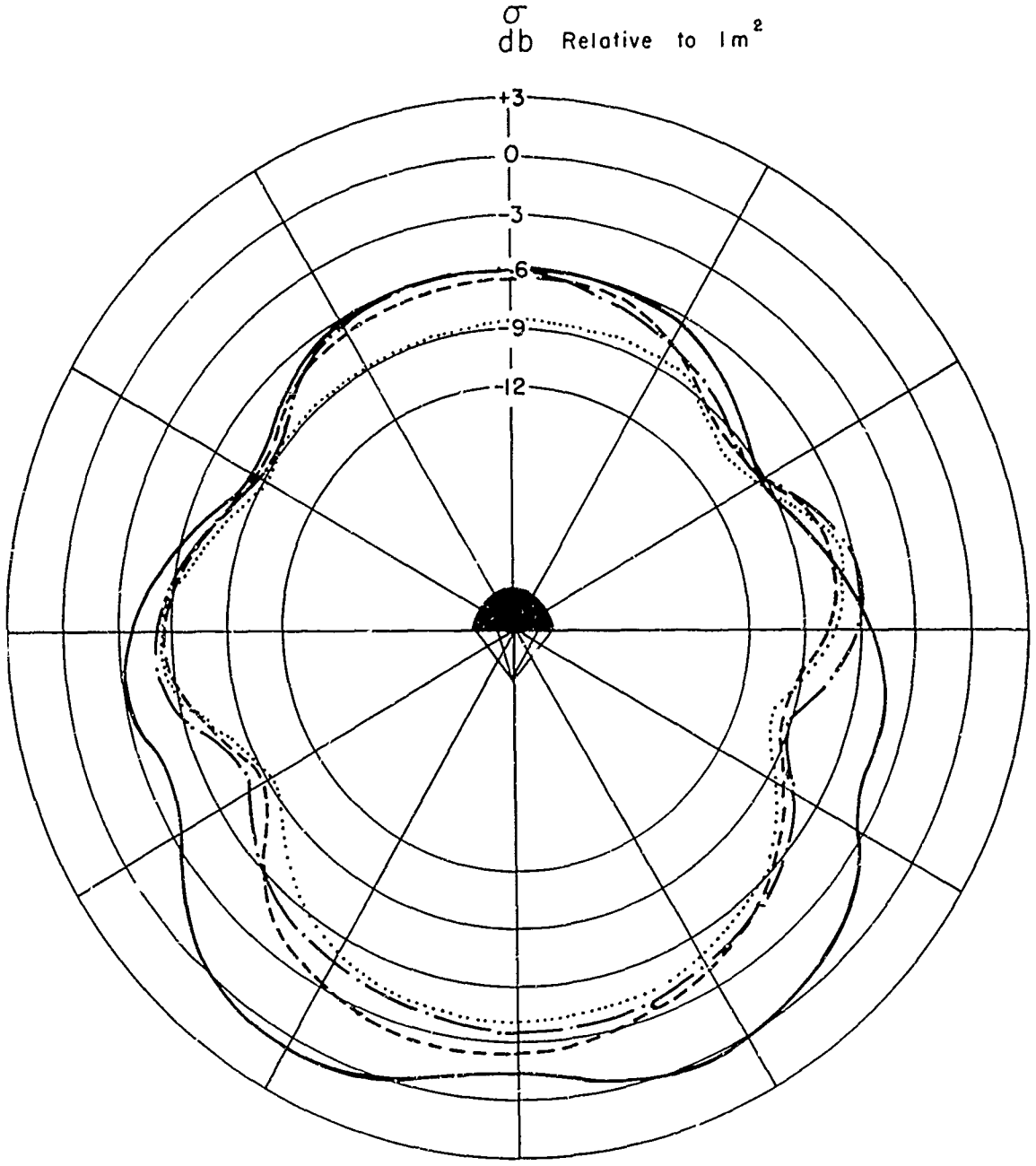

PATTERNS RELATIVE TO TRANSMITTER

—— TRANS & REC ANTENNA SEPARATION 0°
---- " " " " 10°
—·— " " " " 20°
····· " " " " 30°

CURVES ARE MEAN VALUES
SCINTILLATION ± 4 db ABOUT MEAN

PATTERNS OF MODEL PARACHUTE D556.

FIG 16

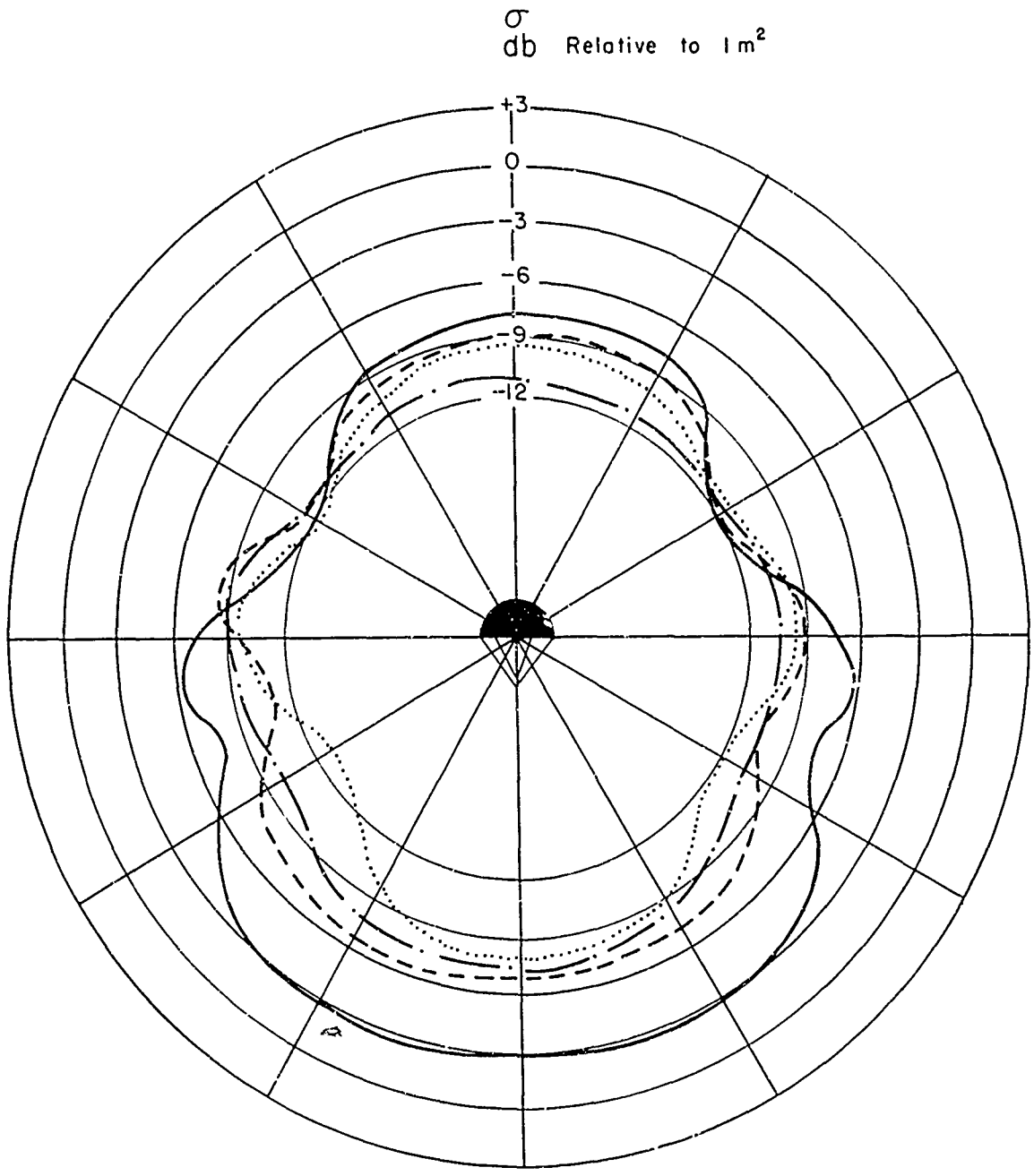

PATTERNS RELATIVE TO TRANSMITTER

——— TRANS & REC ANTENNA SEPARATION 0°
- - - - " " " " 10°
—·— " " " " 20°
..... " " " " 30°

CURVES ARE MEAN VALUES
SCINTILLATION ± 5 db ABOUT MEAN

PATTERNS OF MODEL PARACHUTE D503-6.

FIG 17

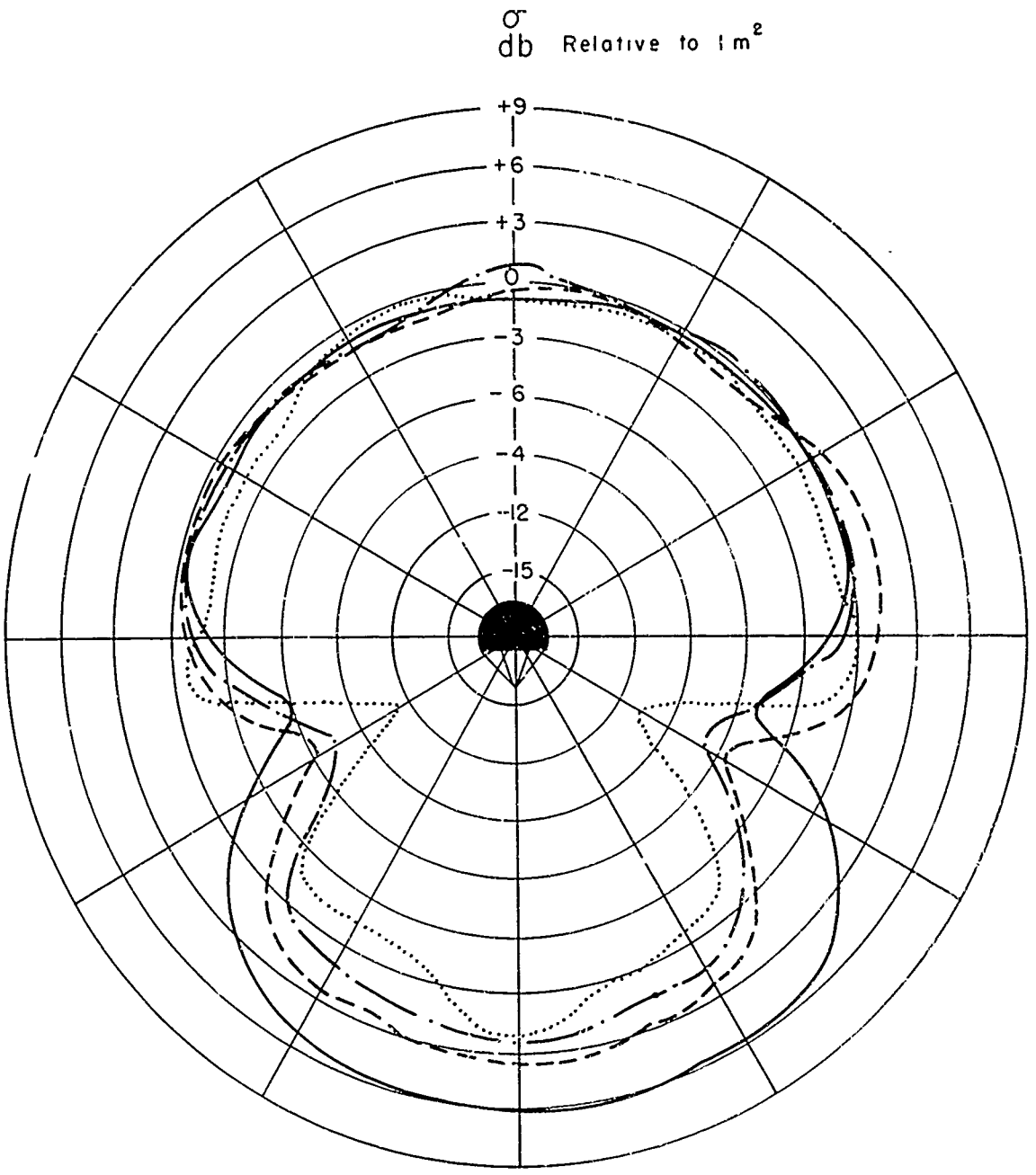

PATTERNS RELATIVE TO TRANSMITTER

——— TRANS & REC. ANTENNA SEPARATION 0°
– – – – " " " " 10°
—·— " " " " 20°
····· " " " " 30°

CURVES ARE MEAN VALUES
SCINTILLATION ± 3 db ABOUT MEAN

PATTERNS OF MODEL PARACHUTE P/N 509-330

FIG. 18

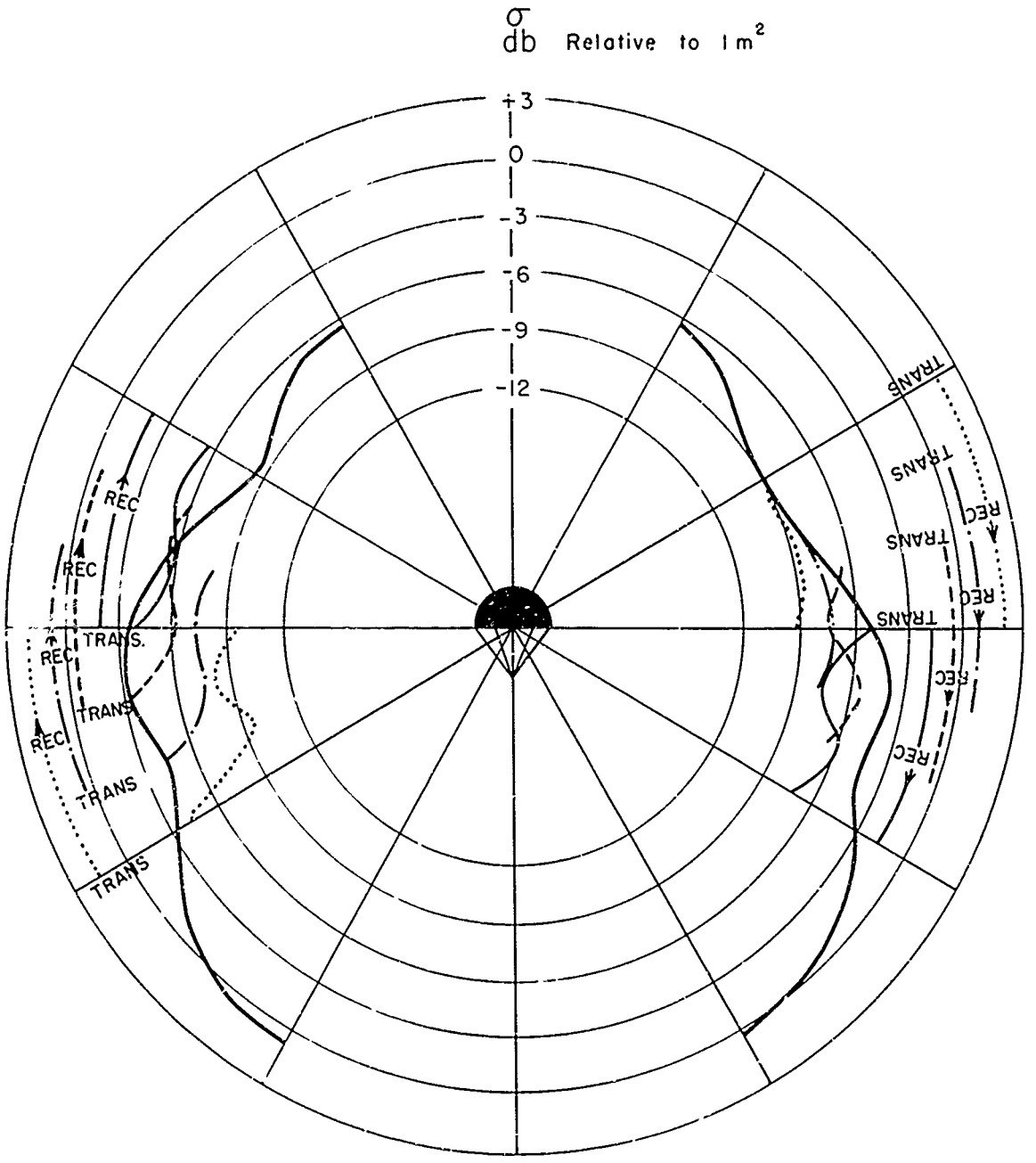

CURVES ARE MEAN VALUES
SCINTILLATION ±5 db ABOUT MEAN

PATTERNS OF FIXED TRANSMITTER & VARYING RECEIVER ASPECT - MODEL PARACHUTE D556.

FIG 19

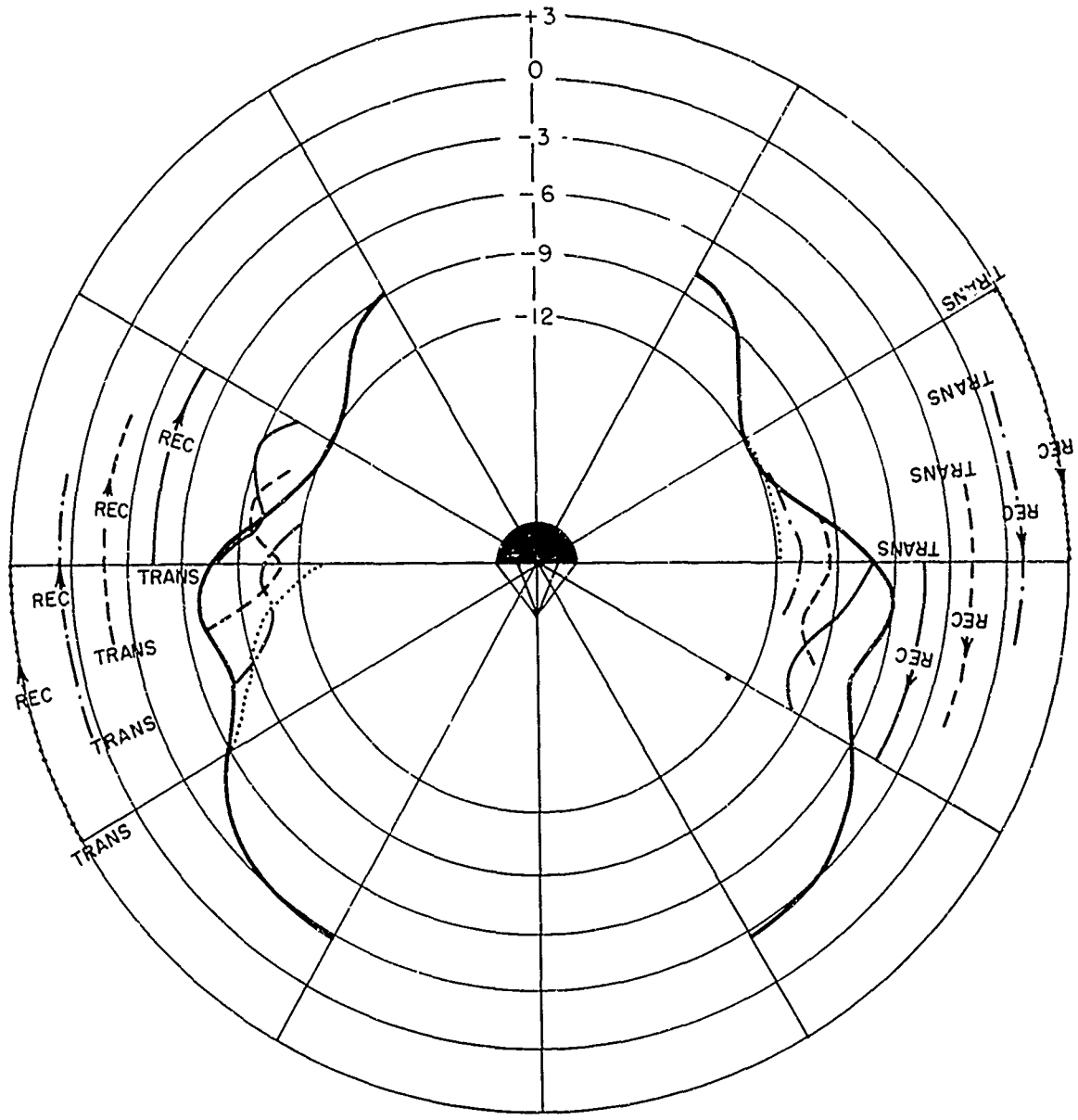

CURVES ARE MEAN VALUES
SCINTILLATION ±5 db ABOUT MEAN

PATTERNS OF FIXED TRANSMITTER & VARYING RECEIVER ASPECT - MODEL PARACHUTE D503-6.

FIG 20

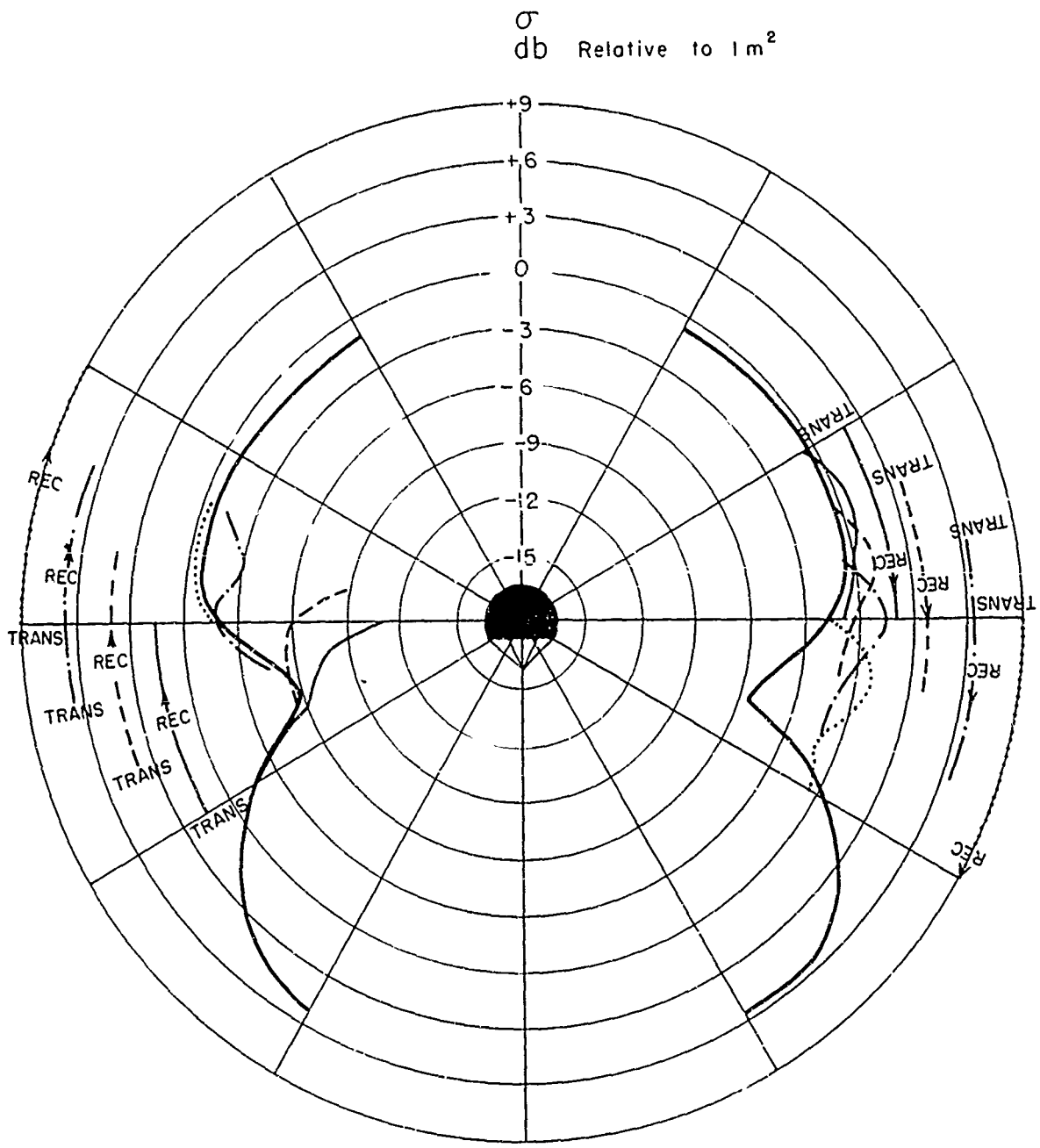

CURVES ARE MEAN VALUES
SCINTILLATION ±3 db ABOUT MEAN

PATTERNS OF FIXED TRANSMITTER & VARYING RECEIVER ASPECT - MODEL PARACHUTE P/N 509-330

FIG 21